Nonlinear Distortion Mitigation via Coherent All-Optical Reservoir Computing for Long-Haul IM-DD transmission Systems

Guanju Peng
Key Laboratory of Opto-electronic Information Technology of Ministry of Education and Tianjin Key Laboratory of Integrated Opto-electronics Technologies and Devices
School of Precision Instruments and Opto-electronics Engineering
Tianjin University
Tianjin, China
guanjup@tju.edu.cn

Yaping Liu*
Key Laboratory of Opto-electronic Information Technology of Ministry of Education and Tianjin Key Laboratory of Integrated Opto-electronics Technologies and Devices
School of Precision Instruments and Opto-electronics Engineering
Tianjin University
Tianjin, China
liuyp@tju.edu.cn

Zheng Li
Key Laboratory of Opto-electronic Information Technology of Ministry of Education and Tianjin Key Laboratory of Integrated Opto-electronics Technologies and Devices
School of Precision Instruments and Opto-electronics Engineering
Tianjin University
Tianjin, China
zhemglee@tju.edu.cn

Kunpeng Zhu
Key Laboratory of Opto-electronic Information Technology of Ministry of Education and Tianjin Key Laboratory of Integrated Opto-electronics Technologies and Devices
School of Precision Instruments and Opto-electronics Engineering
Tianjin University
Tianjin, China
zkp@tju.edu.cn

Zhiqun Yang
Key Laboratory of Opto-electronic Information Technology of Ministry of Education and Tianjin Key Laboratory of Integrated Opto-electronics Technologies and Devices
School of Precision Instruments and Opto-electronics Engineering
Tianjin University
Tianjin, China
yangzhiqun@tju.edu.cn

Janping Li
HMN Technologies Co., Ltd
Tianjin, China
lijianping@hmntechnologies.com

Shigui Zhang
HMN Technologies Co., Ltd
Tianjin, China
sigurd.zhang@hmntechnologies.com

Zhanhua Huang
Key Laboratory of Opto-electronic Information Technology of Ministry of Education and Tianjin Key Laboratory of Integrated Opto-electronics Technologies and Devices
School of Precision Instruments and Opto-electronics Engineering
Tianjin University
Tianjin, China
zhanhua@tju.edu.cn

Lin Zhang*
Key Laboratory of Opto-electronic Information Technology of Ministry of Education and Tianjin Key Laboratory of Integrated Opto-electronics Technologies and Devices
School of Precision Instruments and Opto-electronics Engineering
Tianjin University
Tianjin, China
Peng Cheng Laboratory
Shenzhen, China
lin_zhang@tju.edu.cn

***Abstract*—Photonic reservoir computing (RC), as a promising paradigm of optical signal processing, has attracted a great deal of attention in fiber nonlinearity equalization recently. For real long-haul transmission scenarios, we propose an all-optical RC operated in a coherent scheme to mitigate the nonlinear distortion of high-speed signals. Compared with the direct decision architecture, the proposed RC can dramatically improve the Q^2 factor by 2.6 dB for a single-wavelength system and 1.9 dB for a 7-channel wavelength-division multiplexing (WDM) system over 3960-km fiber transmission. Furthermore, the robustness of the coherent all-optical RC is also verified by conducting studies on different training sequences. The coherent all-optical RC shows great potential in real-time nonlinearity mitigation for long-haul fiber transmissions.**

Keywords—photonic reservoir computing, optical fiber communication, long-haul transmission, nonlinear equalization

I. INTRODUCTION

The exponential growth of internet traffic in this big data era yields new challenges for optical transmission systems, such as ultra-long distance and ultra-high capacity. One straightforward way to overcome the incoming capacity crunch is to increase launch power to improve signal-to-noise ratio (SNR). However, due to the nonlinear Shannon limit, the signal distortions originated from the interactions of chromatic dispersion (CD), Kerr nonlinearity, and amplified spontaneous emission (ASE) noise essentially limit the system capacity of long-haul optical communications. To mitigate the impact of nonlinear signal distortions, digital signal processing (DSP) technologies are widely applied, such as digital back-propagation algorithm [1] and Volterra nonlinear equalizers [2]. Recently, with the development of artificial intelligence (AI) and machine learning, artificial neural networks have become popular in the field of fiber nonlinearity equalization in optical fiber transmission due to their outstanding ability to fit arbitrary functions [3], [4]. However, note that these DSP technologies and electronic neural networks are both offline algorithms, which demand massive computing resources and huge power consumption, limiting their practical use. To solve these challenges, photonic neural networks (PNNs) based on micro-ring resonators with their low latency and efficient power consumption have been proposed to mitigate nonlinear signal distortions [5]. However, the weights in the PNNs should be first obtained by training using a computer, which inevitably

This work was supported by National Key R&D Program of China under grant 2019YFA0706300 and National Natural Science Foundation of China under grant 62105241.

increases the computation and operation complexity with the E/O conversion.

Reservoir computing (RC), which stems from recurrent neural networks (RNN) [6] has attracted great attention in information processing for its simple architecture and fast training procedure [7]. RC generally consists of three parts: an input layer, a reservoir, and a readout layer. The input signal is firstly masked in the input layer to increase its diversity. Then, the masked signals are put into the reservoir to be mapped high-dimension nonlinear states. Finally, the readout signals are weighted and summed to obtain a target signal. It should be noted that the weights in the input layer and the reservoir are fixed, and only the weights in the readout layer are trained by ridge regression, which greatly simplifies the RC process [8]. RC can be implemented using various physical hardware, such as analog circuits [9], dynamic memristors [10], and photonic devices [11]-[18].

Compared with the other two types of RC, photonic RC systems have great advantages of fast computation speed and low power consumption [11], [12], and they have been applied in many different tasks, such as the NARMA 10 task, isolated spoken digit recognition, and nonlinear equalization. Due to superior nonlinear-fitting ability, photonic RC shows great potential in optical fiber communication to mitigate the signal distortion caused by fiber nonlinearity [13]-[16]. However, existing studies mainly focus on the transmission systems with high launch powers to intentionally enhance nonlinearity and exhibit the possibility of RC which are affected by high nonlinear noise and low linear noise, and cannot consider the interaction of CD, Kerr nonlinearity, and ASE noise. Nevertheless, it may not be applicable to real long-haul transmission systems where signals are greatly affected by the interaction of CD, Kerr nonlinear, and ASE noise, which is more difficult to be mitigated than the short reach system. In fact, from a viewpoint of long-haul transmission in practice, fiber communication systems have been designed with a quite low launch power, because it has become well-known in fiber communication community that nonlinear noise is a limiting factor of system performance and hard to handle using DSP. In this sense, till now the effectiveness of RC for nonlinear equalization in real long-haul transmission scenarios remains unclear.

Moreover, photonic RCs with various architectures have been studied, which are based on semiconductor lasers [13], multimode interferometers [14], microrings [15], and Mach-Zehnder modulators [16], but the masks of the above reservoirs are all achieved by electronic devices, in which optical-electrical-optical (O/E/O) conversion is required and inevitably constrains the processing speed of the RCs. In particular, if signal stretching is needed, it will limit the use of RC in real-time communication systems.

Here, we propose a coherent all-optical RC to mitigate the nonlinearity-induced distortion in long-haul transmission. A single-wavelength system and a wavelength-division multiplexing (WDM) system with 7 channels are studied. In the proposed RC, O/E/O conversion is eliminated by the all-optical mask, enabling data to be directly processed in the optical domain, and significantly improving the processing speed. Furthermore, the phase property of the optical signal adjusted by a phase shifter is adopted, which enriches the characteristics of the RC signal and further improves the RC performance.

II. PRINCIPLE AND MODELING

We compare the structure of the proposed coherent all-optical reservoir with the traditional O/E/O-conversion-necessary photonic reservoir in Fig. 1. Due to the masks can be directly achieved in the optical domain, the coherent all-optical RC offers ultra-fast signal processing speed. The long-haul transmission system with the coherent all-optical RC, as shown in Fig. 2, consists of multiple spans, where each span contains a single-mode fiber (SMF) and a dispersion-compensating fiber (DCF). The DCF with negative chromatic dispersion completely compensates for the whole dispersion accumulated within a single span [17].

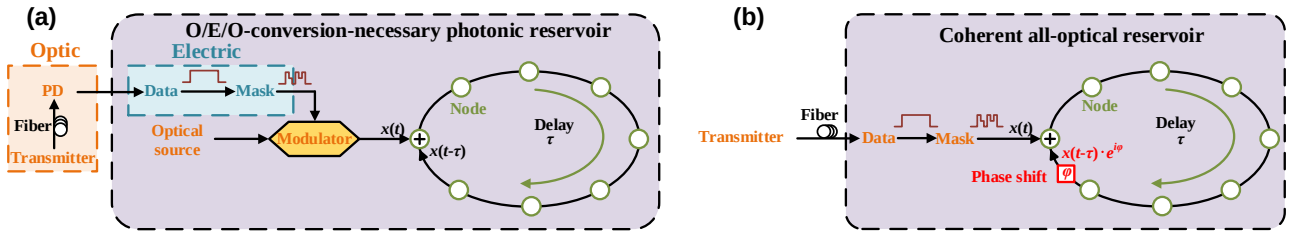

Fig. 1. The schematic of reservoir in optical fiber communication. (a) A traditional O/E/O-conversion-necessary photonic reservoir, in which O/E/O conversion is required to achieve the masks, inevitably constrains the processing speed of the RC. (b) The proposed coherent all-optical reservoir, in which the all-optical mask eliminates O/E/O conversion to significantly improve the processing speed and the phase property of the feedback optical signal adjusted by a phase shifter to enrich the characteristics of the RC signal.

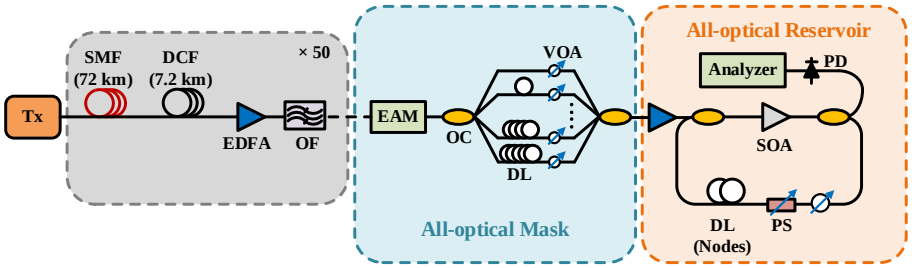

Fig. 2. The schematic of a long-haul transmission system based on the coherent all-optical RC. This system consists of three parts: the transmission link, the all-optical mask, and the all-optical reservoir. Tx: transmitter; SMF: single-mode fiber; DCF: dispersion-compensating fiber; EDFA: erbium-doped fiber amplifier; OF: optical filter; EAM: electro-absorption modulator; OC: optical coupler; DL: delay line; VOA: variable optical attenuator; SOA: semiconductor optical amplifier; PS: phase shifter; PD: photodetector.

After long-haul transmission, signal crosstalk caused by chromatic dispersion can be limited within several symbols, significantly reducing the complexity of the RC. An erbium-doped fiber amplifier (EDFA) is used to compensate for the power loss of each span, and an optical filter (OF) filters out the noise outside the channel.

After long-haul transmission, the signal is directly reshaped in the optical domain by an electro-absorption modulator (EAM) which serves as an optical gate. This process eliminates the need for O/E/O conversion and can be regarded as a method of all-optical signal processing [18]. Each symbol can pass through the EAM only over a time duration, $\Delta\tau$, when the EAM driver signal is on. Then, the signal is split into N branches and propagates via delay lines (DLs) with increasing delays nT/N (n = 0, …, N-1), where T is the symbol time. Variable optical attenuators (VOAs) are used to mask the transmitted signal and increase its diversity. After a combiner, the masked signal is injected into an all-optical reservoir to mitigate nonlinearity in the fiber transmission. An EDFA is used to change the signal power injected into the reservoir consisting of a nonlinear node, i.e., a semiconductor optical amplifier (SOA), a VOA, a phase shifter (PS), and a DL. The SOA implements the nonlinearity transform of the masked signal. The VOA and PS change the strength and the phase of the feedback signal, respectively. The virtual reservoir nodes are implemented by the DL to induce interactions between adjacent symbols.

To gain a deep insight into the reservoir, we show the signal flow in Fig. 3. The signal $\beta \cdot m_k u(n)$ after the all-optical mask is mixed with the feedback signal $\alpha \cdot x_{k-j}(n\text{-}1) \cdot e^{i(\varphi+\varphi_D)}$ and passes through the SOA nonlinear function $f(x)$ to generate the signal $x_k(n) = f(\beta \cdot m_k u(n) + \alpha \cdot x_{k-j}(n\text{-}1) \cdot e^{i(\varphi+\varphi_D+\pi/2)})$, where β is the gain of the EDFA in front of the reservoir, m_k is the mask in the k_{th} branch, $u(n)$ is the signal passing through the EAM, α is the attenuation of the VOA, φ is the phase of signal adjusted by the PS, φ_D is the phase introduced by virtual nodes, and the subscript j is the difference between the number of virtual nodes and masks, j = 0, …, N-1. Note that, in the reservoir, the duration time of a virtual node is set to T/N, and the total number of virtual nodes is N + j.

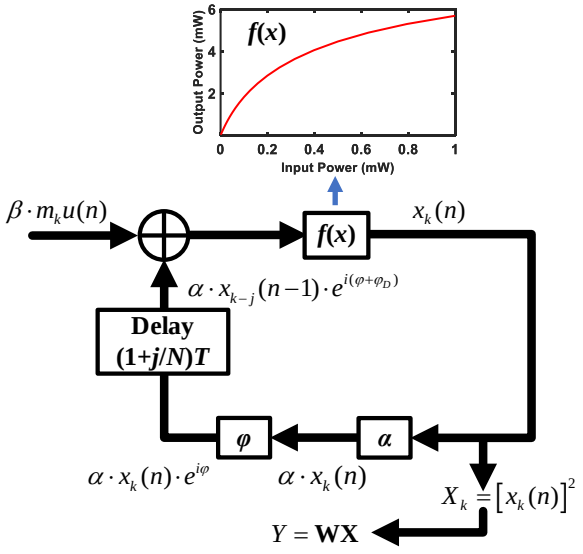

Fig. 3. The schematic of signal flow in the all-optical reservoir. The signal phase information is included in the reservoir to enrich the characteristics of the proposed RC. At the output port, ridge regression is used to obtain the eqaulized signal.

At the output port of the reservoir, a part of the signal is split from the reservoir and received by the PD that responds to the power rather than the field amplitude. Subsequently, the received signal vector, **X**, are multiplied with the output weight vector, **W**, to obtain the target signal, Y, for nonlinearity mitigation. Here, **W** is derived from the ridge regression at the training stage, i.e., $\mathbf{W}=(\mathbf{X}^{\mathrm{T}}\mathbf{X}+\lambda\mathbf{I})^{-1}\mathbf{X}^{\mathrm{T}}Y$, where λ is the ridge coefficient and **I** is an identity matrix. The other part of the signal is fed back into the reservoir, and finally the delayed signal is added with the incoming signal to generate the signal that once again enters the reservoir. By deriving the expression of the signal circulating in a photonic reservoir, one can have a chance to compare it to those based on other physical mechanisms in the future and gain a better understanding on the functionalities of RC.

III. RESULTS

Different nonlinear effects have different influences on a system's performance. In a single-wavelength system, the signal is mainly influenced by self-phase modulation (SPM). While in a wavelength-division multiplexing (WDM) system, cross-phase modulation (XPM) and four-wave mixing (FWM) are the dominant nonlinear effect. Here, we study the RC performance on both a single-wavelength system and a 7-channel WDM system.

A. The RC performance in a single-wavelength system

First, a single-wavelength system with the above coherent all-optical RC is studied using VPI Photonics Transmission Maker. At the transmitter, a pseudo-random bit sequence (PRBS) of 2^{18} bits is generated and mapped into a 28-GBaud NRZ-OOK signal at 1550 nm. The transmission link consists of 50 spans, where each span contains a 72-km SMF and a 7.2-km DCF. The SMF has a chromatic dispersion of 17 ps/nm/km, a loss of 0.2 dB/km, and a nonlinear index of 2.6×10^{-20} m^2/W. The DCF's dispersion, loss, and nonlinear index are -170 ps/nm/km, 0.6 dB/km, and 2.3×10^{-20} m^2/W, respectively [17]. The noise figure of the EDFA is 5 dB, the optical bandwidth of the OF is 112 GHz, and the total transmission length is 3960 km. Meanwhile, eight branches are adopted to mask the distorted signal in the all-optical mask. In the reservoir, the number of virtual nodes is determined by the delay time. As the interval of each virtual node equals to the duration of each masked signal, i.e., T/8, a longer delay time means more virtual nodes. The processed signal is received by a PD with 8 samples per symbol.

In order to obtain the optimum performance on fiber nonlinearity compensation, we optimize key parameters in the RC, such as the number of symbols employed in the ridge regression algorithm, the mask pattern determined by eight VOAs in the all-optical mask, the VOA attenuation, the EDFA gain, the phase shift, and the number of virtual nodes

TABLE I. OPTIMUM PARAMETERS IN THE RC

Parameter	Value
Number of symbols	11
Mask pattern	1,1,1,0,1,1,1,1
VOA attenuation	14 dB
EDFA gain	31 dB
Phase shift	160°
Number of virtual nodes	9

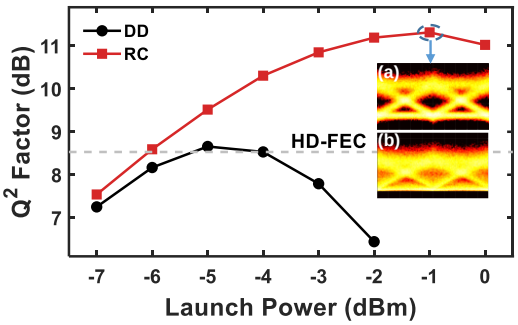

Fig. 4. Q^2 factor versus launch power under the direct decision (DD) and the RC. The inset (a) and (b) are the eye diagrams of the RC and the DD at the launch power of -1 dBm, respectively. The optimum Q^2 factors of the DD and the RC are 8.7 dB at the launch power of -5 dBm and 11.3 dB at the launch power of -1 dBm, respectively.

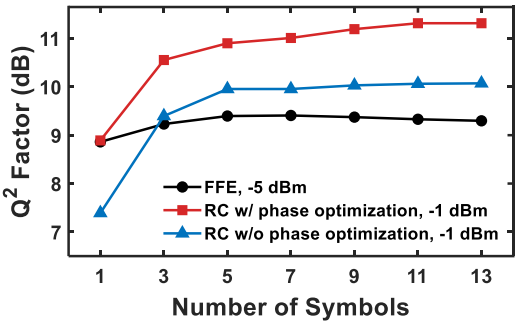

Fig. 5. The performance comparison among the feed-forward equalizer (FFE) and the RC with and without phase optimization. The RC with phase optimization, i.e., the proposed coherent RC, obtains the best performance, showing great improvements in the Q2 factor. Specifically, it outperforms the FFE by 1.9 dB and the RC without phase optimization by 1.1 dB.

in the reservoir. Here, we take Q^2 factors to characterize the performance of the RC, which can be derived from the bit error ratio (BER): $Q^2=20\log_{10}[\sqrt{2}\mathrm{erfc}^{-1}(2\mathrm{BER})]$ [2]. By a joint sweep of the above parameters, we obtain a set of these optimum parameters of the RC, as given in TABLE I.

Figure 3 shows the Q^2 factor as a function of the launch power under the optimum parameters in TABLE I. Because the signal power injected into the reservoir can be changed at different launch power, we adjust the gain synchronously to vary RC performance. It can be found that the optimum Q^2 factors of the direct decision (DD) and the RC are 8.7 dB at the launch power of -5 dBm and 11.3 dB at the launch power of -1 dBm, respectively. There is a great improvement in the Q2 factor, as high as 2.6 dB, enabled by the RC.

Feed-forward equalizer (FFE) is widely used to eliminate inter-symbol interference (ISI) in IM-DD systems [19]. Here, we further observe the Q^2-factor improvement by applying the FFE at the launch power of -5 dB dBm for the DD. To eliminate the ISI, multiple symbols are utilized, with each symbol consisting of 8 samples. As shown in Fig. 4, the optimum Q^2 factor of FFE increases to 9.4 dB, with an improvement of 0.7 dB over the DD. Notably, the optimum Q^2 factor of the RC with phase optimization, i.e., 11.3 dB, is still 1.9 dB higher than that after FFE. However, when we remove the phase shifter, the RC performs poorly due to breaking the phase coherence, resulting in a relatively low Q^2 factor of 10.1 dB. It means that the phase shifter plays a crucial role in maintaining phase coherence, which is vital for optimal performance in the RC.

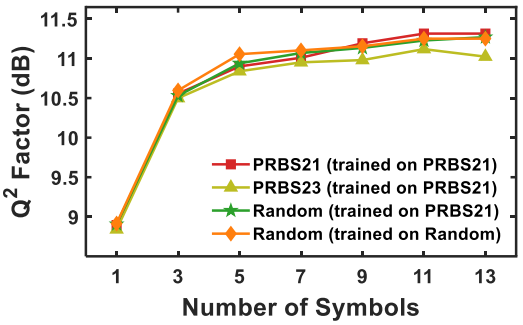

Fig. 6. The RC performance under different signal sequences. The Q^2 factors after the RC are greater than 11 dB in all cases, indicating that the RC has good robustness to different input signal types.

The RC is a variant of recurrent neural networks, which has powerful learning ability but may have a risk of overfitting [20]. To verify the robustness of the proposed RC, we change the types of input for training and testing. Different cases are studied: (I) a PRBS-21 data for training and another PRBS-21 data for testing, (II) a PRBS-21 data for training and a PRBS-23 data for testing, (III) a PRBS-21 data for training and a random data for testing, and (IV) a random data for training and another random data for testing. Fig. 5 shows that the Q^2 factors after the RC are greater than 11 dB in all cases, indicating that the RC has good robustness to different input signal types. It can be interpreted that the noises in the system, from EDFAs in the fiber link and the SOA and PD in the RC, can break the inherent characteristics of the PRBS sequences, thus reducing the risk of overfitting in the RC.

B. The RC performance in a WDM system

To further study the effectiveness of the proposed RC on inter-channel nonlinear mitigation, a WDM system with 7

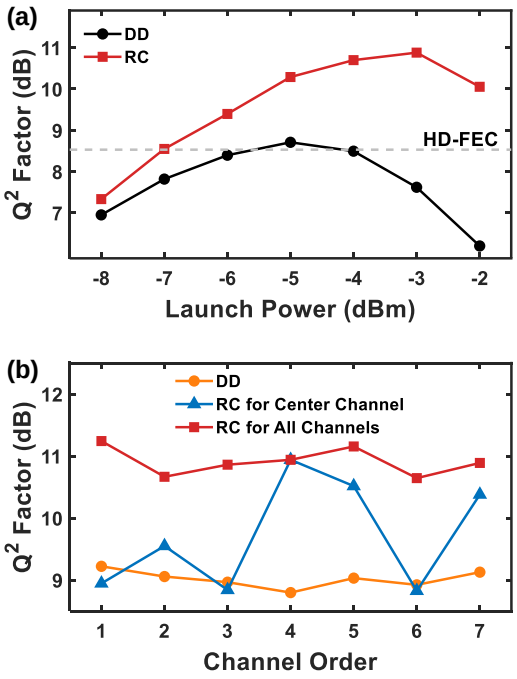

Fig. 7. The RC performance on the 7-channel WDM system. (a) Q^2 factor versus launch power at the central channel, a 2.1 dB improvement can be obtained by the RC. (b) Q^2 factor in different optimization approaches for all channels. When the RC is optimized separately for each channel, the Q^2 factors in all channels have an average improvement of 1.9 dB.

TABLE II. OPTIMUM PARAMETERS IN THE RC FOR EACH CHANNEL

Channel order / Parameter	Channel1	Channel2	Channel3	Channel4	Channel5	Channel6	Channel7
Number of symbols	11	11	11	11	11	11	11
Mask pattern	1,1,0,0,1,0,0,0	1,1,0,1,0,1,0,0	1,0,0,1,1,0,1,1	1,1,1,0,1,1,1,1	1,0,1,0,1,0,0,0	0,0,1,1,0,1,0,1	1,0,1,1,1,0,0,0
VOA attenuation	18 dB	14 dB	18 dB	14 dB	13 dB	13 dB	12 dB
EDFA gain	30 dB	29 dB	31 dB	31 dB	31 dB	32 dB	32 dB
Phase shift	160°	90°	170°	160°	150°	160°	160°
Number of virtual nodes	9	9	9	9	9	9	9

channels is studied in the same way as the above single-λ system. We number the 7 channels from the smallest to the largest according to the channel frequency, and the central channel at 1550 nm is defined as No. 4. The channel space is 50 GHz and the symbol rate is 28 GBaud. Here, the optimum parameters in the RC for every channel are shown in TABLE II. We see that the optimum parameters for equalizing the central channel are the same as above. In Fig. 6(a), the RC obtains the best performance of 10.9-dB Q^2 factor at the launch power of -3 dBm, while the best performance of the DD is obtained at the launch power of -5 dBm with a Q^2 factor of 8.8 dB. There is a great improvement in the Q^2 factor, as high as 2.1 dB, enabled by the RC. It indicates that the proposed RC is not only able to compensate for the SPM but also able to mitigate the inter-channel XPM and FWM in the WDM system.

Besides, we present the RC performance on all channels in Fig. 6(b). For the DD, the Q^2 factor is low everywhere. For the RC, two cases are studied: (I) RC for the central channel, i.e., the RC has a fixed set of optimum parameters obtained from the central channel, and (II) RC for all channels, i.e., the RC has a different set of parameters optimized separately for each channel. We find that the RC in case (I) cannot ensure good performance on the other channels. This is mainly attributed to the coherent property of our RC and the dispersion-induced wavelength dependence of the signal phase. When we optimize the parameters separately for each channel, the Q^2 factors in all channels have an average improvement of 1.9 dB. It means that our RC also performs well in mitigating the XPM and FWM effects for all channels.

IV. CONCLUSION

For the first time, we propose and demonstrate a coherent all-optical RC to mitigate the nonlinear distortion in long-haul transmission systems over 3960-km fibers. By comparing the DD architecture, we find that the proposed RC can dramatically improve the Q^2 factor by 2.6 dB for the single-wavelength system and 1.9 dB for the 7-channel WDM system. With appropriate phase adoption, the RC performance can improve from 10.1 dB to 11.3 dB in the single-wavelength system. Furthermore, the robustness of the coherent all-optical RC is also verified by conducting studies on different training sequences. Due to the data processing in the all-optical domain, the proposed coherent all-optical RC paves the way to real-time fiber nonlinearity equalization in long-haul optical fiber communication systems.

V. REFERENCES

[1] J. Zhang, X. Li and Z. Dong, "Digital nonlinear compensation based on the modified logarithmic step size," J. Lightw. Technol., vol. 31, no. 22, pp. 3546-3555, Nov. 2013.

[2] L. Liu et al., "Intrachannel nonlinearity compensation by inverse Volterra series transfer function," J. Lightw. Technol., vol. 30, no. 3, pp. 310–316, Feb. 2012.

[3] Z. Wan et al.,. "Nonlinear equalization based on pruned artificial neural networks for 112-Gb/s SSB-PAM4 transmission over 80-km SSMF," Opt. Exp., vol. 26, no. 8, pp. 10631-10642, Apr. 2018.

[4] Z. Xu, C. Sun, T. Ji, J. H. Manton, and W. Shieh, "Feedforward and recurrent neural network-based transfer learning for nonlinear equalization in short-reach optical links," J. Lightw. Technol., vol. 39, no. 2, pp. 475–480, Jan. 2021.

[5] C. Huang *et al.*, "A silicon photonic–electronic neural network for fibre nonlinearity compensation," Nat. Electron., vol. 4, no. 11, pp. 837–844, Nov. 2021.

[6] H. Jaeger and H. Haas, "Harnessing nonlinearity: Predicting chaotic systems and saving energy in wireless communication," *Science*, vol. 304, no. 5667, pp. 78–80, Apr. 2004.

[7] M. Lukoševičius, and H. Jaeger, "Reservoir computing approaches to recurrent neural network training," Comput. Sci. Rev., vol. 3, no. 3, pp. 127–149, Aug. 2009.

[8] S. Ortín, "A unified framework for reservoir computing and extreme learning machines based on a single time-delayed neuron," Sci. Rep., vol. 5, no. 14945, pp. 1–11, Oct. 2015.

[9] C. Miguel *et al.*, "Delay-based reservoir computing: noise effects in a combined analog and digital implementation," *IEEE Trans. Neural Netw. Learn. Syst.*, vol. 26, no. 2, pp. 388–393, Feb. 2015.

[10] C. Du *et al.*, "Reservoir computing using dynamic memristors for temporal information processing," *Nat. Commun.*, vol. 8, no. 2204, pp. 1–10, Dec. 2017.

[11] Y. Paquot *et al.*, "Optoelectronic Reservoir Computing," *Sci. Rep.*, vol. 2, no. 1, pp. 1–6, Feb. 2012.

[12] Y. Chen *et al.*, "Reservoir computing system with double optoelectronic feedback loops," *Opt. Exp.*, vol. 27, no. 20, pp. 27431–27440, Sep. 2019.

[13] A. Argyris, J. Bueno, and I. Fischer, "PAM-4 transmission at 1550 nm using photonic reservoir computing post-processing," *IEEE Access*, vol. 7, pp. 37017–37025, Apr. 2019.

[14] S. Sackesyn, C. Ma, J. Dambre, and P. Bienstman, "Experimental realization of integrated photonic reservoir computing for nonlinear fiber distortion compensation," Opt. Exp., vol. 29, no. 20, pp. 30991–30997, Sep. 2021.

[15] S. Li, S. Dev, S. Kühl, K. Jamshidi, and S. Pachnicke, "Micro-ring resonator based photonic reservoir computing for PAM equalization," IEEE Photon. Technol. Lett., vol. 32, no. 18, pp. 978–981, Jun. 2021.

[16] S. Wang, N. Fang, and L. Wang, "Signal recovery based on optoelectronic reservoir computing for high speed optical fiber communication system," Opt. Commun., vol. 495, no. 15, pp. 1–7, Sep. 2021.

[17] L. Gruner-Nielsen et al., "Dispersion-compensating fibers," J. Lightw. Technol., vol. 23, no. 11, pp. 3566–3579, Nov. 2005.

[18] H. Tanaka, T. Otani, M. Hayashi, and M. Suzuki, "Optical signal processing with electro-absorption modulators," in OFC 2002 Tech. Dig., Anaheim, CA, USA, 2002, pp. 262–264.

[19] P.M. Watts *et al.*, "Performance of single-mode fiber links using electronic feed-forward and decision feedback equalizers," *IEEE Photon. Technol. Lett.*, vol. 17, no. 10, pp. 2206–2208, Sep. 2005.

[20] L. Yi et al., "Machine learning for 100 Gb/s/λ passive optical network," J. Lightw. Technol., vol. 37, no. 6, pp. 1621–1630, Mar. 2019.